Quasiparticle random phase approximation based on the relativistic Hartree-Bogoliubov model. II. Nuclear spin and isospin excitations

Paar, Nils; Nikšić, Tamara; Vretenar, Dario; Ring, Peter

Quasiparticle random phase approximation based on the relativistic Hartree-Bogoliubov model. II. Nuclear spin and isospin excitations

N. Paar
Institut für Kernphysik, Technische Universität Darmstadt, Schlossgartenstrasse 9, D-64289 Darmstadt, Germany

T. Nikšić and D. Vretenar
Physics Department, Faculty of Science, University of Zagreb, Croatia, and Physik-Department der Technischen Universität München, D-85748 Garching, Germany

P. Ring
Physik-Department der Technischen Universität München, D-85748 Garching, Germany

(Received 24 February 2004; published 10 May 2004)

The proton-neutron relativistic quasiparticle random-phase approximation (PN-RQRPA) is formulated in the canonical single-nucleon basis of the relativistic Hartree-Bogoliubov model, for an effective Lagrangian characterized by density-dependent meson-nucleon couplings. The model includes both the $T=1$ and $T=0$ pairing channels. Pair configurations formed from the fully or partially occupied states of positive energy in the Fermi sea, and the empty negative-energy states from the Dirac sea, are included in PN-RQRPA configuration space. The model is applied to the analysis of charge-exchange modes: isobaric analog resonances and Gamow-Teller resonances.

DOI: 10.1103/PhysRevC.69.054303 PACS number(s): 21.30.Fe, 21.60.Jz, 24.30.Cz, 25.40.Kv

I. INTRODUCTION

A consistent and unified treatment of mean-field and pairing correlations is crucial for a quantitative analysis of ground-state properties and multipole response of unstable, weakly bound nuclei far from the line of β stability. In Ref. [1] we have formulated the relativistic quasiparticle random-phase approximation (RQRPA) in the canonical single-nucleon basis of the relativistic Hartree-Bogoliubov (RHB) model. The RHB model presents the relativistic extension of the Hartree-Fock-Bogoliubov framework, and it provides a unified description of particle-hole (ph) and particle-particle (pp) correlations. In this framework the ground state of a nucleus can be written either in the quasiparticle basis as a product of independent quasiparticle states, or in the canonical basis as a highly correlated BCS state. By definition, the canonical basis diagonalizes the density matrix and it is always localized. It describes both the bound states and the positive-energy single-particle continuum. The formulation of the RQRPA in the canonical basis is particularly convenient because, in order to describe transitions to low-lying excited states in weakly bound nuclei, the two-quasiparticle configuration space must include states with both nucleons in the discrete bound levels, states with one nucleon in a bound level and one nucleon in the continuum, and also states with both nucleons in the continuum.

The relativistic QRPA of Ref. [1] is fully self-consistent. For the interaction in the particle-hole channel effective Lagrangians with nonlinear meson self-interactions are used, and pairing correlations are described by the pairing part of the finite range Gogny interaction. Both in the ph and pp channels, the same interactions are used in the RHB equations that determine the canonical quasiparticle basis, and in the matrix equations of the RQRPA. The RQRPA configuration space includes also the Dirac sea of negative energy states. The RHB+RQRPA approach has been tested in the example of multipole excitations of neutron rich oxygen isotopes, and the model has been employed in the analysis of the evolution of the low-lying isovector dipole strength in Sn isotopes and $N=82$ isotones.

Relativistic mean-field and RPA calculations based on effective Lagrangians with nonlinear meson self-interactions present not only a number of technical problems, but also the description of finite nuclei obtained with these effective interactions is not satisfactory, especially for isovector properties. As an alternative, in a number of recent applications models with density-dependent meson-nucleon vertex functions have been used. Although the two classes of models are essentially based on the same microscopic structure, i.e., on density-dependent interactions, the latter can be more directly related to the underlying microscopic nuclear interactions. Several recent analyses have shown that relativistic effective interactions with explicit density dependence of the meson-nucleon couplings provide an improved description of asymmetric nuclear matter, neutron matter and nuclei far from stability. In Ref. [2] we have extended the RHB model to include density-dependent meson-nucleon couplings. The effective Lagrangian is characterized by a phenomenological density dependence of the σ, ω, and ρ meson-nucleon vertex functions, adjusted to properties of nuclear matter and finite nuclei. It has been shown that, in comparison with standard relativistic mean-field (RMF) effective interactions with nonlinear meson-exchange terms, the new density-dependent meson-nucleon force DD-ME1 significantly improves the description of asymmetric nuclear matter and of ground-state properties of $N\neq Z$ nuclei. This is, of course, very important for the extension of RMF-based models to exotic nuclei far from β stability, and for applications in the field of nuclear astrophysics.

In Ref. [3] the matrix equations of the relativistic random-phase approximation (RRPA) have been derived for an effective Lagrangian characterized by density-dependent meson-nucleon couplings. The explicit density dependence introduces rearrangement terms in the residual two-body interaction, and their contribution is essential for a quantitative description of excited states. Illustrative calculations of the isoscalar monopole, isovector dipole and isoscalar quadrupole response of ^{208}Pb, were performed in the fully self-consistent RRPA framework based on effective interactions with a phenomenological density dependence adjusted to nuclear matter and ground-state properties of spherical nuclei.

In this work we extend the model developed in Ref. [1], and formulate a proton-neutron relativistic QRPA in the canonical single-nucleon basis of the RHB model. The proton-neutron RQRPA, with the density-dependent effective interaction DD-ME1, will be employed in the analysis of nuclear spin and isospin excitations.

Collective spin and isospin excitations in atomic nuclei have been the subject of many experimental and theoretical studies (for an extensive review see Ref. [4]). Nucleons with spin up and spin down can oscillate either in phase (spin scalar $S=0$ mode) or out of phase (spin vector $S=1$ mode). The spin vector, or spin-flip excitations can be of isoscalar ($S=1$, $T=0$) or isovector ($S=1$, $T=1$) nature. These collective modes provide direct information on the spin and spin-isospin dependence of the effective nuclear interaction.

Especially interesting is the collective spin-isospin oscillation with the excess neutrons coherently changing the direction of their spins and isospins without changing their orbital motion—the Gamow-Teller resonance (GTR) $J^{\pi}=1^{+}$. This collective mode was predicted already in 1963 [5], but it was only in 1975 that the first experimental indications of the GT resonance were observed in (p,n) charge-exchange reactions at intermediate energies [6]. The detailed knowledge of GT strength distributions is essential for the understanding of nuclear reactions in the process of nucleosynthesis. In particular, the low-lying GT strength is directly related to β-decay rates, as well as to the electron-capture process leading to the stellar collapse and supernovae explosion. In many nuclei all over the periodic table the GT strength distribution, when measured in the excitation energy region where the most pronounced GT peaks occur, is quenched by more than 20% when compared to a model independent sum rule. Two physically different mechanisms had been suggested as a possible explanation of the quenching of the total GTR strength: (i) nuclear configuration mixing—the high-lying $2p$-$2h$ states mix with the $1p$-$1h$ GT states and shift the GT strength to high-energy region far beyond the resonance [7–9]; (ii) the high-energy Δ-isobar—nucleon-hole configurations (Δ-h) couple to the GT mode and remove part of the strength from the low-lying excitation spectrum [10,11]. Recent (p,n) scattering experiments have shown, however, that only a small fraction of the GT quenching originates from Δ-h transitions [12].

The GT spin-flip isovector excitations and the related β decays have been theoretically investigated by employing: (i) the shell-model approach, (ii) the nonrelativistic proton-neutron quasiparticle random-phase approximation, and (iii) the relativistic random-phase approximation in closed-shell nuclei. Experimental data on charge-exchange excitations in light and medium-mass nuclei are very successfully reproduced by large-scale shell-model calculations. However, as the number of valence nucleons increases, the dimension of shell-model configuration space becomes far too large for practical calculations. Shell-model calculations have been recently extended to the region of pf-shell nuclei with $A=45-65$. Experimental Gamow-Teller strength distributions and nuclear β-decay half-lives have been reproduced [13]. The GT response in medium-mass nuclei has also been successfully described by shell-model Monte Carlo calculations (SMMC) [14].

The proton-neutron quasiparticle random-phase approximation (PN-QRPA) can be used to describe nuclei in mass regions that are presently beyond the reach of the most sophisticated shell-model calculations. The pioneering work of Halbleib and Sorensen [15] was based on simple separable forces. Further developments employed zero-range interactions with BCS-type pairing. Most studies of GT excitations have been based on Skyrme interactions [16–20]. It has also been shown that the inclusion of particle-particle correlations in the QRPA residual interaction has an important effect in the calculation of β-decay rates [21–26].

Experimental data on unstable nuclei close to $N=Z$ line, that became available in recent studies with radioactive beams, have also renewed the interest in the role of proton-neutron pairing. In medium-heavy and heavy nuclei closer to the line of β stability, the proton and neutron Fermi levels are located in different major shells, and therefore the contribution of proton-neutron pairing correlations to the ground-state binding is usually neglected. The low-lying GT strength responsible for β-decay, however, involves proton-neutron particle-particle correlations and is sensitive to the $T=0$ pairing interaction. In Ref. [26] β-decay rates for spherical neutron-rich r-process waiting-point nuclei have been calculated within a fully self-consistent QRPA, formulated in the Hartree-Fock-Bogoliubov canonical single-particle basis. It has been shown that the proton-neutron particle-particle interaction has a pronounced effect on the calculated half-lives.

Surprisingly little work has been reported on the description of charge-exchange excitations in finite nuclei in the framework of relativistic mean-field models. The first relativistic RPA calculations of isobaric analog resonances (IAR) and Gamow-Teller resonances have been performed only recently in Refs. [27,28]. This analysis was, however, restricted to doubly closed-shell nuclei. A rather small configuration space was used and, furthermore, configurations that include empty states from the negative-energy Dirac sea were neglected. In a very recent work [29] it has been shown, on the other hand, that the inclusion of negative-energy Dirac sea states has a pronounced effect on the calculated Gamow-Teller sum rule. A more complete relativistic RPA calculation of GT resonances in doubly closed-shell nuclei has been reported in Ref. [30]. The ground states of ^{48}Ca, ^{90}Zr, and ^{208}Pb were calculated in the RMF model with the NL3 effective interaction. The spin-isospin correlations in the RRPA calculation of the GT response functions were induced by the isovector mesons π and ρ. In addition to the

standard nonlinear NL3 effective interaction [31] with the vector rho-nucleon coupling, the effective Lagrangian included the pseudo-vector pion-nucleon interaction. Although in the relativistic mean-field description of the nuclear ground state the direct one-pion contribution vanishes at the Hartree level because of parity conservation, the pion nevertheless plays an important role for excitations that involve spin degrees of freedom. Since it has a relatively small mass, the pion mediates the effective nuclear interaction over large distances. The *p-h* residual interaction with ρ- and π-meson exchange has been extensively used in non-relativistic RPA calculations of charge-exchange excitations [32,33]. Because of the derivative type of the pion-nucleon coupling, it is also necessary to include a zero-range Landau-Migdal term that accounts for the contact part of the nucleon-nucleon interaction. The analysis of Ref. [30] has shown that the RRPA calculation with the NL3 effective interaction, the pseudo-vector pion-nucleon coupling ($m_\pi = 138$ MeV and $f_\pi^2/4\pi = 0.08$), and the Landau-Migdal force with the strength parameter $g_0' = 0.6$, reproduces the experimental excitation energies of the main components of the GT resonances in ^{48}Ca, ^{90}Zr, and ^{208}Pb.

In Ref. [34] we have calculated the GTR and IAR for a sequence of even-even Sn target nuclei by using the framework of the relativistic Hartree-Bogoliubov model plus proton-neutron quasiparticle random-phase approximation. The calculation reproduces the experimental data on ground-state properties, as well as the excitation energies of the isovector excitations. It has been shown that the isotopic dependence of the energy spacings between the GTR and IAR provides direct information on the evolution of neutron skin thickness along the Sn isotopic chain. A new method has been suggested for determining the difference between the radii of the neutron and proton density distributions along an isotopic chain, based on measurement of the excitation energies of the GTR relative to the IAR.

This work presents a much more detailed analysis of charge-exchange modes, both for doubly closed-shell and for open-shell nuclei. In Sec. II we introduce the formalism. The matrix equations of the proton-neutron relativistic QRPA are formulated in the canonical basis of the RHB model for spherical nuclei. In Sec. III the RHB+RQRPA model is employed in illustrative calculations of charge-exchange collective modes: isobaric analog resonances and Gamow-Teller resonances. Section IV contains the conclusions.

II. PROTON-NEUTRON RELATIVISTIC QUASIPARTICLE RANDOM-PHASE APPROXIMATION

In Ref. [1] we have derived the RQRPA from the time-dependent RHB model in the limit of small amplitude oscillations. The full RQRPA equations are rather complicated and it is considerably simpler to solve these equations in the canonical basis, in which the relativistic Hartree-Bogoliubov wave functions can be expressed in the form of BCS-like wave functions. In this case one needs only the matrix elements $V^{ph}_{\kappa\lambda'\kappa'\lambda}$ of the residual ph interaction, and the matrix elements $V^{pp}_{\kappa\kappa'\lambda\lambda'}$ of the pairing pp interaction, as well as certain combinations of the occupation factors u_κ, v_κ. The details of the RHB model, of the RQRPA formalism, and the technicalities of the solution of the RQRPA equations in the canonical basis, are given in Ref. [1]. In this section we only collect those expressions which are specific for the PN-RQRPA. The model can be considered as a relativistic extension of the fully-consistent proton-neutron QRPA formulated in Ref. [26], and applied in an analysis of β-decay rates of *r*-process nuclei.

We consider transitions between the 0^+ ground state of a spherical even-even parent nucleus and the J^π excited state of the corresponding odd-odd daughter nucleus. These transitions are induced by a charge-exchange operator T^{JM}. Taking into account the rotational invariance of the nuclear system, the quasiparticle pairs can be coupled to good angular momentum and the matrix equations of the PN-RQRPA read

$$\begin{pmatrix} A^J & B^J \\ B^{*J} & A^{*J} \end{pmatrix} \begin{pmatrix} X^{\lambda J} \\ Y^{\lambda J} \end{pmatrix} = E_\lambda \begin{pmatrix} 1 & 0 \\ 0 & -1 \end{pmatrix} \begin{pmatrix} X^{\lambda J} \\ Y^{\lambda J} \end{pmatrix}. \tag{1}$$

The matrices A and B are defined in the canonical basis [35]

$$\begin{aligned} A^J_{pn,p'n'} = {} & H^{11}_{pp'}\delta_{nn'} + H^{11}_{nn'}\delta_{pp'} + (u_p v_n u_{p'} v_{n'} \\ & + v_p u_n v_{p'} u_{n'}) V^{phJ}_{pn'np'} + (u_p u_n u_{p'} u_{n'} \\ & + v_p v_n v_{p'} v_{n'}) V^{ppJ}_{pnp'n'}, \end{aligned}$$

$$\begin{aligned} B^J_{pn,p'n'} = {} & (-1)^{j_{p'}-j_{n'}+J}(u_p v_n v_{p'} u_{n'} + v_p u_n u_{p'} v_{n'}) V^{phJ}_{pp'nn'} \\ & - (u_p u_n v_{p'} v_{n'} + v_p v_n u_{p'} u_{n'}) V^{ppJ}_{pnp'n'}. \end{aligned} \tag{2}$$

Here p, p', and n, n' denote proton and neutron quasiparticle canonical states, respectively, V^{ph} is the proton-neutron particle-hole residual interaction, and V^{pp} is the corresponding particle-particle interaction. The canonical basis diagonalizes the density matrix and the occupation amplitudes $v_{p,n}$ are the corresponding eigenvalues. The canonical basis, however, does not diagonalize the Dirac single-nucleon mean-field Hamiltonian $\hat{h}_D$ and the pairing field $\hat{\Delta}$, and therefore the off-diagonal matrix elements $H^{11}_{nn'}$ and $H^{11}_{pp'}$ appear in Eq. (2):

$$H^{11}_{\kappa\kappa'} = (u_\kappa u_{\kappa'} - v_\kappa v_{\kappa'}) h_{\kappa\kappa'} - (u_\kappa v_{\kappa'} + v_\kappa u_{\kappa'}) \Delta_{\kappa\kappa'}. \tag{3}$$

For each energy E_λ, $X^{\lambda J}$ and $Y^{\lambda J}$ in Eq. (2) denote the corresponding forward- and backward-going QRPA amplitudes, respectively. The total strength for the transition between the ground state of the even-even (N,Z) nucleus and the excited state of the odd-odd $(N+1,Z-1)$ or $(N-1,Z+1)$ nucleus, induced by the operator T^{JM}, reads

$$B^\pm_{\lambda J} = \left| \sum_{pn} < p \| T^J \| n > (X^{\lambda J}_{pn} u_p v_n + (-1)^J Y^{\lambda J}_{pn} v_p u_n) \right|^2. \tag{4}$$

The discrete strength distribution is folded by the Lorentzian function

$$R(E)^{\pm} = \sum_{\lambda} B^{\pm}_{\lambda J} \frac{1}{\pi} \frac{\Gamma/2}{(E - E_{\lambda_{\pm}})^2 + (\Gamma/2)^2}. \tag{5}$$

In the illustrative calculations included in the following sections, the choice for the width of the Lorentzian function is 1 MeV.

The spin-isospin dependent interaction terms are generated by the ρ- and π-meson exchange. Because of parity conservation, the one-pion direct contribution vanishes in the mean-field calculation of a nuclear ground state. Its inclusion is important, however, in calculations of excitations that involve spin and isospin degrees of freedom. The particle-hole residual interaction in the PN-RQRPA is derived from the Lagrangian density

$$\mathcal{L}^{int}_{\pi+\rho} = -g_{\rho} \overline{\psi} \gamma^{\mu} \vec{\rho}_{\mu} \vec{\tau} \psi - \frac{f_{\pi}}{m_{\pi}} \overline{\psi} \gamma_5 \gamma^{\mu} \partial_{\mu} \vec{\pi} \vec{\tau} \psi. \tag{6}$$

Vectors in isospin space are denoted by arrows, and boldface symbols will indicate vectors in ordinary three-dimensional space.

The coupling between the ρ meson and the nucleon is assumed to be a vertex function of the vector density $\rho_v = \sqrt{j_{\mu} j^{\mu}}$, with $j_{\mu} = \overline{\psi} \gamma_{\mu} \overline{\psi}$. In Ref. [3] it has been shown that the explicit density dependence of the meson-nucleon couplings introduces additional rearrangement terms in the residual two-body interaction of the RRPA, and that their contribution is essential for a quantitative description of excited states. However, since the rearrangement terms include the corresponding isoscalar ground-state densities, it is easy to see that they are absent in the charge exchange channel, and the residual two-body interaction reads

$$V(\boldsymbol{r}_1, \boldsymbol{r}_2) = \vec{\tau}_1 \vec{\tau}_2 (\beta \gamma^{\mu})_1 (\beta \gamma_{\mu})_2 g_{\rho}[\rho_v(\boldsymbol{r}_1)] g_{\rho}[\rho_v(\boldsymbol{r}_2)] D_{\rho}(\boldsymbol{r}_1, \boldsymbol{r}_2) - \left(\frac{f_{\pi}}{m_{\pi}} \right)^2 \vec{\tau}_1 \vec{\tau}_2 (\boldsymbol{\Sigma}_1 \boldsymbol{\nabla}_1)(\boldsymbol{\Sigma}_2 \boldsymbol{\nabla}_2) D_{\pi}(\boldsymbol{r}_1, \boldsymbol{r}_2). \tag{7}$$

$D_{\rho(\pi)}$ denotes the meson propagator

$$D_{\rho(\pi)} = \frac{1}{4\pi} \frac{e^{-m_{\rho(\pi)} |\boldsymbol{r}_1 - \boldsymbol{r}_2|}}{|\boldsymbol{r}_1 - \boldsymbol{r}_2|}, \tag{8}$$

and

$$\boldsymbol{\Sigma} = \begin{pmatrix} \boldsymbol{\sigma} & 0 \\ 0 & \boldsymbol{\sigma} \end{pmatrix}. \tag{9}$$

For the ρ-meson coupling we adopt the functional form used in the DD-ME1 density-dependent effective interaction [2]

$$g_{\rho}(\rho_v) = g_{\rho}(\rho_{sat}) \exp[-a_{\rho}(x-1)], \tag{10}$$

where $x = \rho_v / \rho_{sat}$, and ρ_{sat} denotes the saturation vector nucleon density in symmetric nuclear matter. For the pseudovector pion-nucleon coupling we use the standard values

$$m_{\pi} = 138.0 \text{ MeV}, \quad \frac{f_{\pi}^2}{4\pi} = 0.08. \tag{11}$$

The derivative type of the pion-nucleon coupling necessitates the inclusion of the zero-range Landau-Migdal term, which accounts for the contact part of the nucleon-nucleon interaction

$$V_{\delta\pi} = g' \left(\frac{f_{\pi}}{m_{\pi}} \right)^2 \vec{\tau}_1 \vec{\tau}_2 \boldsymbol{\Sigma}_1 \cdot \boldsymbol{\Sigma}_2 \delta(\boldsymbol{r}_1 - \boldsymbol{r}_2), \tag{12}$$

with the parameter $g' \approx 0.6$ adjusted to reproduce experimental data on the GTR excitation energies.

With respect to the RHB calculation of the ground state of an even-even nucleus, the charge-exchange channel includes the additional one-pion exchange contribution. The PN-RQRPA model is fully consistent: the same interactions, both in the particle-hole and particle-particle channels, are used in the RHB equation that determines the canonical quasiparticle basis, and in the PN-RQRPA equation (1). In both channels the same strength parameters of the interactions are used in the RHB and RQRPA calculations.

The two-quasiparticle configuration space includes states with both nucleons in the discrete bound levels, states with one nucleon in the bound levels and one nucleon in the continuum, and also states with both nucleons in the continuum. In addition to the configurations built from two-quasiparticle states of positive energy, the RQRPA configuration space contains pair-configurations formed from the fully or partially occupied states of positive energy and the empty negative-energy states from the Dirac sea. As will be shown in the following section, the inclusion of configurations built from occupied positive-energy states and empty negative-energy states is essential for the consistency of the model.

Nuclear properties calculated with the RHB plus RQRPA model depend on the choice of the effective RMF Lagrangian in the ph channel, as well as on the treatment of pairing correlations. In this work, for the RHB calculation of ground states and in the ph channel of the residual interaction, we use the density-dependent effective interaction DD-ME1. In Ref. [2] the RHB model with the density-dependent interaction DD-ME1 in the ph channel, and with the finite range Gogny interaction D1S in the pp channel, has been tested in the analysis of the equations of state for symmetric and asymmetric nuclear matter, and of ground-state properties of the Sn and Pb isotopic chains. It has been shown that, as compared to standard nonlinear relativistic mean-field effective forces, the interaction DD-ME1 has better isovector properties and therefore provides an improved description of asymmetric nuclear matter, neutron matter and nuclei far from stability.

In the pp channel of the RHB model we have used a phenomenological pairing interaction, the pairing part of the Gogny force,

$$V^{pp}(1,2) = \sum_{i=1,2} e^{-[(\boldsymbol{r}_1 - \boldsymbol{r}_2)/\mu_i]^2} (W_i + B_i P^{\sigma} - H_i P^{\tau} - M_i P^{\sigma} P^{\tau}), \tag{13}$$

with the set D1S [36] for the parameters μ_i, W_i, B_i, H_i, and $M_i (i = 1, 2)$. This force has been very carefully adjusted to the

pairing properties of finite nuclei all over the periodic table. In particular, the basic advantage of the Gogny force is the finite range, which automatically guarantees a proper cutoff in momentum space. In the present analysis we will also use the Gogny interaction in the $T=1$ pp channel of the PN-RQRPA. For the $T=0$ proton-neutron pairing interaction in open shell nuclei we employ a similar interaction: a short-range repulsive Gaussian combined with a weaker longer-range attractive Gaussian,

$$V_{12} = -V_0 \sum_{j=1}^{2} g_j e^{-r_{12}^2/\mu_j^2} \hat{\Pi}_{S=1,T=0}, \tag{14}$$

where $\hat{\Pi}_{S=1,T=0}$ projects onto states with $S=1$ and $T=0$. This interaction was used in the nonrelativistic QRPA calculation [26] of β-decay rates for spherical neutron-rich r-process waiting-point nuclei. As it was done in Ref. [26], we take the ranges $\mu_1=1.2$ fm and $\mu_2=0.7$ fm of the two Gaussians from the Gogny interaction (13), and choose the relative strengths $g_1=1$ and $g_2=-2$ so that the force is repulsive at small distances. The only remaining free parameter is V_0, the overall strength.

III. CHARGE-EXCHANGE COLLECTIVE MODES OF EXCITATIONS

A. The isobaric analog resonance

The IAR presents the simplest charge-exchange excitation mode, detected already forty years ago in experiments on low-energy proton elastic scattering from heavy nuclei. The observed resonances were at energies consistent with the interpretation that they were isobaric analog states in the compound nucleus. One of the important characteristics of an IAR is its narrow width. This is because it has the same isospin as the parent state, while the neighboring states have the isospin of the ground state of the daughter nucleus, i.e., they differ in isospin by one unit. This means that they will couple only weakly with the IAR.

As a first test of our PN-RQRPA model, we calculate the IAR strength functions, i.e., the distribution of $J^\pi=0^+$. The Fermi transition operator reads

$$T^F_{\beta^\pm} = \sum_{i=1}^{A} \tau_\pm. \tag{15}$$

In Fig. 1 we display the PN-RRPA response to the operator (15) for ^{48}Ca, ^{90}Zr, and ^{208}Pb. The strength distributions are dominated by a single IAR peak, which corresponds to a coherent superposition of $\pi p-\nu h$ (or proton-neutron $2qp$) excitations. The calculated excitation energies (evaluated with respect to the ground state of the parent nucleus) are compared with the corresponding experimental values (thick arrows) from (p,n) scattering data for ^{48}Ca [37], ^{90}Zr [12,38], and ^{208}Pb [39]. The agreement between the PN-RRPA and experimental data is indeed very good. We have also verified that the calculated strength distributions exhaust the Fermi nonenergy weighted sum rule

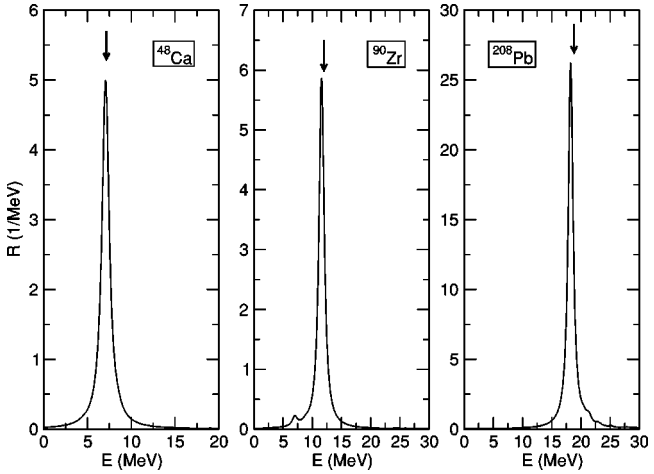

FIG. 1. PN-RQRPA $J^\pi=0^+$ strength distributions. The excitations of the isobaric analog resonances are compared with experimental data (thick arrows) for ^{48}Ca [37], ^{90}Zr [12,38], and ^{208}Pb [39].

$$S_{\beta^-}(F) = N - Z. \tag{16}$$

The proton-neutron relativistic QRPA provides a natural framework for the description of spin and isospin excitations in open-shell nuclei. In Fig. 2 we plot the calculated IAR excitation energies for the sequence of even-even Sn target nuclei with $A=108-132$. The result of fully self-consistent RHB plus proton-neutron RQRPA calculations are shown in comparison with experimental data obtained in a systematic study of the $(^3\mathrm{He},t)$ charge-exchange reaction over the entire range of stable Sn isotopes [40]. The calculated values reproduce the empirical mass dependence of the IAR excitation energies, and we also notice a very good agreement with available experimental data. For the nuclei with $A=112-124$ the largest difference between the theoretical and experimental IAR excitation energies is $\approx$200 keV. For the Sn nuclei with $A=108-132$, in Figs. 3 and 4 we display the corresponding theoretical strength

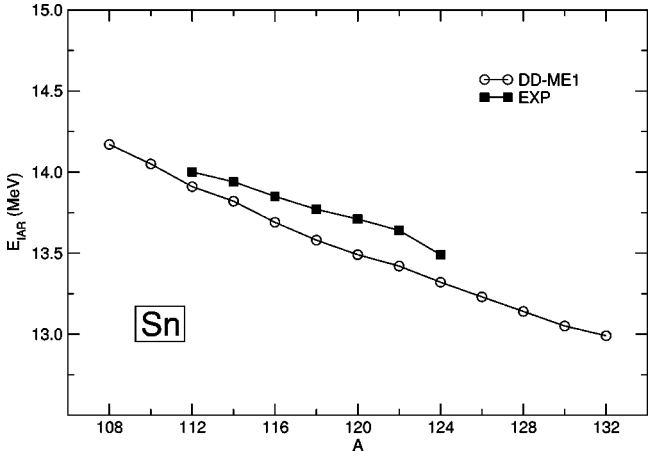

FIG. 2. RHB plus proton-neutron RQRPA results for the isobaric analog resonances of the sequence of even-even Sn target nuclei. The experimental data are from Ref. [40].

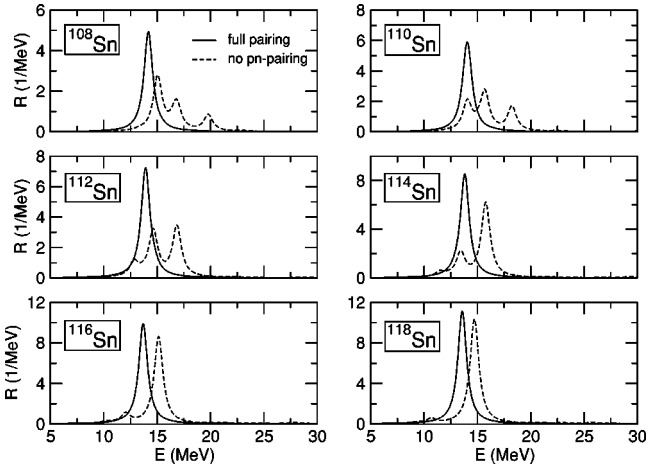

FIG. 3. PN-RQRPA $J^{\pi}=0^{+}$ strength distributions for even-even Sn target nuclei with $A=108-118$. For description see text.

distribution functions. To illustrate the importance of a consistent treatment of pairing correlations, in addition to the response functions calculated with the fully self-consistent RHB plus proton-neutron RQRPA, we also display the strength functions obtained without including the proton-neutron residual pairing interaction. Proton-neutron pairing, of course, does not contribute in the RHB calculation of the ground states. The dashed curves are calculated by including only the ph channel of the RQRPA residual interaction. In both cases (solid and dashed curves) $T=1$ neutron-neutron pairing has been included in the RHB calculations of the ground-states of Sn target nuclei. The results shown in Figs. 3 and 4 clearly illustrate the pronounced effect that $T=1$ proton-neutron pairing correlations have on the calculated IAR. Without proton-neutron pairing the calculated IAR excitation energies for nuclei with $A\geqslant 116$ are simply too high. The attractive proton-neutron pairing interaction redistributes the strength between various QRPA components, and lowers the calculated excitation energy to the value which corresponds to the difference between the Coulomb energies of the target nucleus and the $(Z+1,N-1)$ daughter nucleus. As one would expect, the effect gradually weakens as the closed shell at $N=82$ is approached. The effect of the proton-neutron residual pairing on the IAR strength distributions in lighter Sn isotopes with $A\leqslant 114$ is more dramatic. Without the contribution of the pp channel to the proton-neutron residual interaction, the response function is fragmented and it does not display the experimentally observed single narrow resonance. Only with the inclusion of proton-neutron pairing a single collective state is obtained.

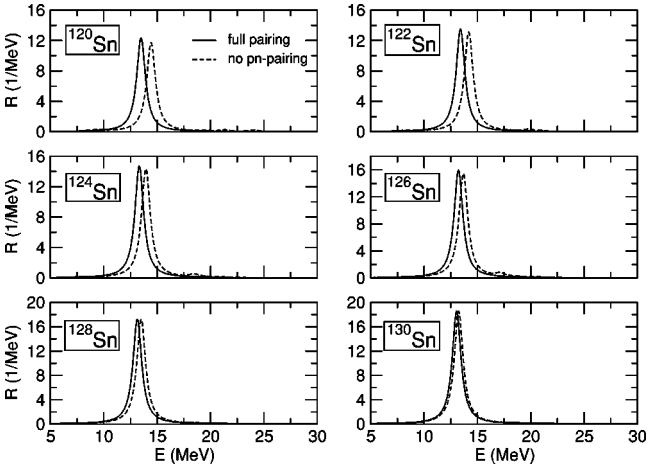

FIG. 4. Same as in Fig. 3, for even-even Sn target nuclei with $A=120-130$.

The mechanism through which the PN-RQRPA builds the IAR in Sn isotopes is illustrated in Fig. 5 for ^{108}Sn, ^{114}Sn, and ^{120}Sn. The figure displays the discrete QRPA spectra for the following three cases. In the panels on the left we plot the spectra calculated without any pairing interaction, either in calculation of the ground state, or in the residual proton-neutron interaction. It is immediately clear why the three particular examples were selected. Without pairing, the $g_{7/2}$ neutron orbital is fully occupied in the ground state of ^{108}Sn, the $g_{7/2}$ and the $d_{5/2}$ orbitals are fully occupied in the ground state of ^{114}Sn, and for ^{120}Sn all the neutron orbitals in the shell $N=50-82$ are occupied, except $h_{11/2}$. For all three nuclei the response function to the Fermi operator (15) displays a single peak at the excitation energy very close to the experimental position of the IAR. The distribution of neutron-to-proton RPA amplitudes is shown next to each major peak. For example, in the case of ^{108}Sn 99% of the strength results from the transition $\nu\, g_{7/2}\rightarrow \pi\, g_{7/2}$, whereas for ^{120}Sn 98% of the strength is distributed between the four orbitals occupied by the neutrons in the $N=50-82$ shell. In the next step (middle panels in Fig. 5) we include the Gogny neutron-neutron pairing in the RHB calculation of the ground states, and as a result all the $N=50-82$ neutron orbitals acquire finite occupation probabilities. The pp channel, however, is not allowed to contribute to the QRPA matrix elements of the proton-neutron residual interaction. In this case the QRPA spectra become fragmented in ^{108}Sn and ^{114}Sn. Considerable strength is transferred to states which correspond to transitions from neutron orbitals with low occupation probabilities: $s_{1/2}$ and $h_{11/2}$. For the most pronounced peaks we have included the distribution of neutron-to-proton QRPA amplitudes.The fragmentation does not occur in ^{120}Sn where, as a result of ground-state pairing correlations, all the $N=50-82$ neutron orbitals have considerable occupation probabilities. In ^{120}Sn we notice only a redistribution of QRPA amplitudes in favor of higher-lying orbitals, and consequently the repulsive particle-hole residual interaction shifts the IAR to higher energy. For the two nuclei from the lower half of the $N=50-82$ neutron shell, the ph residual interaction fragments the QRPA spectra and effectively precludes the formation of the IAR. The panels on the right-hand side of Fig. 5 display the result obtained by fully-consistent PN-RQRPA calculations, including the $T=1$ proton-neutron pairing channel: the strength has been collected in a single peak—the IAR. We notice that with respect to the case (a) without any pairing correlations, the IAR strength has been redistributed among the neutron-to-proton QRPA amplitudes, reflecting the occupation of higher-lying neutron orbitals in the parent nucleus. The calculated excitation energies, as we have shown in Fig.

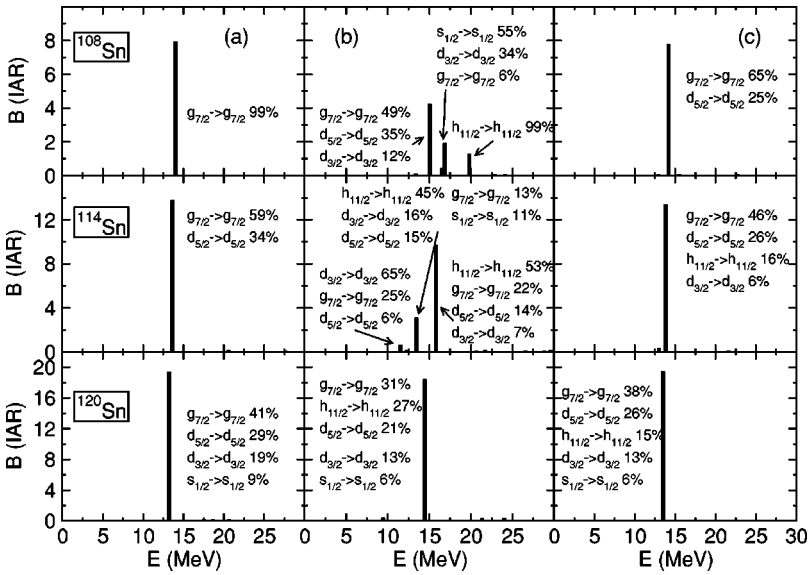

FIG. 5. PN-RQRPA $J^{\pi}=0^{+}$ discrete spectra for ^{108}Sn, ^{114}Sn, and ^{120}Sn. The panels on the left correspond to calculations performed without including pairing correlations. $T=1$ Gogny pairing is included in the RHB calculations of ground states in the middle panels. The panels on the right-hand side display the results obtained by fully-consistent PN-RQRPA calculations, including the $T=1$ proton-neutron pairing channel.

2, are in very good agreement with the experimental data on the IAR in Sn nuclei [40]. The total effect is, of course, simply a consequence of the fact that the pairing interaction is isospin invariant, and therefore commutes with the Fermi operator (15). However, the results shown in Figs. 3–5 illustrate the importance of a consistent treatment of pairing correlations by including an isospin invariant pairing interaction in the description of the ground state and the dynamics of IAR in $N\neq Z$ nuclei.

B. The Gamow-Teller resonance

The Gamow-Teller resonance represents a coherent superposition of high-lying $J^{\pi}=1^{+}$ proton-particle—neutron-hole configurations of maximum collectivity associated with charge-exchange excitations of neutrons from orbitals with $j=l+\frac{1}{2}$ into proton orbitals with $j=l-\frac{1}{2}$. The GT operator reads

$$T^{GT}_{\beta^{\pm}}=\sum_{i=1}^{A}\Sigma\tau_{\pm}. \tag{17}$$

The calculated GT strength distributions for ^{48}Ca, ^{90}Zr, and ^{208}Pb are shown in Fig. 6. In addition to the high-energy GT resonance—a collective superposition of direct spin-flip $\left(j=l+\frac{1}{2}\rightarrow j=l-\frac{1}{2}\right)$ transitions, the response functions display a concentration of strength in the low-energy tail. The transitions in the low-energy region correspond to core-polarization $\left(j=l\pm\frac{1}{2}\rightarrow j=l\pm\frac{1}{2}\right)$, and back spin-flip $\left(j=l-\frac{1}{2}\rightarrow j=l+\frac{1}{2}\right)$ neutron-hole—proton-particle excitations.

As in the calculation of the IAR, the effective RMF interaction is DD-ME1. In addition, the standard values have been used for the parameters of the pion-nucleon interaction Lagrangian: $m_{\pi}=138$ MeV and $f_{\pi}^{2}/4\pi=0.08$, and the parameter of the zero-range Landau-Migdal force $g'=0.55$ has been adjusted to reproduce the excitation energy of the GT resonance in ^{208}Pb. The calculated resonances are shown in comparison with experimental data (thick arrows) for the GTR excitation energies in ^{48}Ca [37], ^{90}Zr [12,38], and ^{208}Pb [39,41,42]. Although the residual interaction has been adjusted to reproduce the GTR excitation energy in ^{208}Pb, we notice a very good agreement with experiment also for ^{48}Ca and ^{90}Zr. The adjusted value of g' in general depends on the choice of the RMF effective interaction. In the RRPA calculation with the NL1 [43] effective interaction of Ref. [27], the GTR excitation energies of ^{48}Ca, ^{90}Zr, and ^{208}Pb were best reproduced by $g'=0.7$, whereas approximately the same quality of agreement with experimental data was obtained in Ref. [30] by using the NL3 [31] effective interaction and $g'=0.6$. By using a set of density-dependent RMF effective interactions from Ref. [3] we have verified that, in general, there is a correlation between the value of the nuclear asymmetry energy at saturation a_4, and the value of g' adjusted to reproduce the GTR. In order to reproduce the experimental excitation energy of the GTR, effective interactions with higher values of a_4 generally require higher values of g'.

Gamow-Teller states calculated in relativistic models have recently attracted considerable attention [29,30,44,45]. In

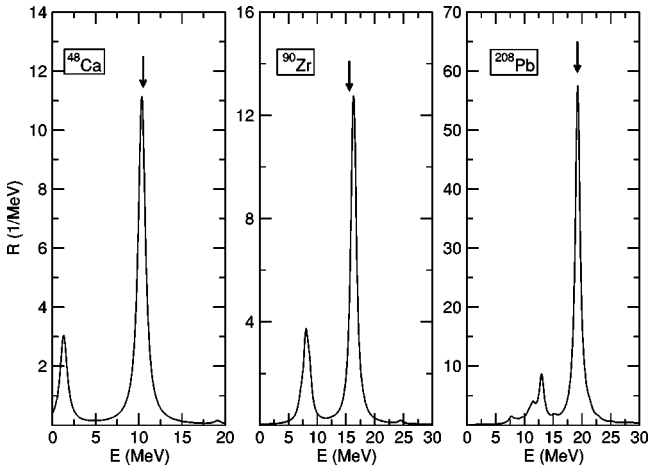

FIG. 6. Gamow-Teller strength distributions for ^{48}Ca, ^{90}Zr, and ^{208}Pb. PN-RQRPA results are shown in comparison with experimental data (thick arrows) for the GTR excitation energies in ^{48}Ca [37], ^{90}Zr [12,38], and ^{208}Pb [39,41,42].

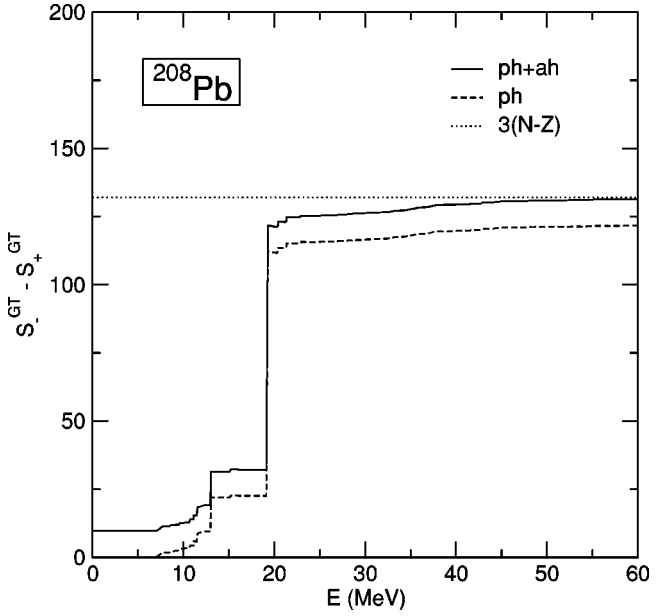

FIG. 7. The running sum of the GTR strength for ^{208}Pb. The dashed line corresponds to a PN-RRPA calculation with only positive-energy ph configurations. For the calculation denoted by the solid line the RRPA space contains configurations formed from occupied states in the Fermi sea and empty negative-energy states in the Dirac sea. The total sum of the GT strength is compared to the model independent Ikeda sum rule (dotted line).

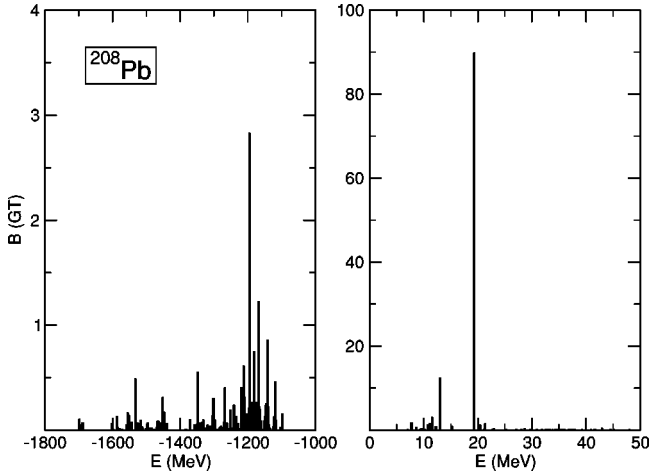

FIG. 8. The PN-RQRPA strength distribution of discrete $J^\pi = 1^+$ GT$^-$ states. The panel on the right-hand side contains the positive energy $\pi p - \nu h$ strength. The left panel displays the negative energy spectrum built from $\pi\alpha - \nu h$ transitions.

particular, it has been shown that in a relativistic RPA calculation the total GT strength in the nucleon sector is reduced by $\approx$12% in nuclear matter, and by $\approx$6% in finite nuclei when compared to the Ikeda sum rule [5]

$$(S^{GT}_{\beta^-} - S^{GT}_{\beta^+}) = 3(N-Z), \tag{18}$$

where $S^{GT}_{\beta^\pm}$ denotes the total sum of Gamow-Teller strength for the $\beta^\pm$ transition. The reduction has been attributed to the effect of Dirac sea negative-energy states, i.e., the missing part of the sum rule is taken by particle-hole excitations formed from ground-state configurations of occupied states in the Fermi sea and empty negative-energy states in the Dirac sea. The effect is illustrated in Fig. 7, where we display the running sum of GTR strength for ^{208}Pb. The horizontal dotted line corresponds to the value $3(N-Z)=132$ of the Ikeda sum rule. The solid and dashed lines corresponds the values of the GTR sum calculated from $-\infty$ to the excitation energy denoted on the abscissa. The big jump in the calculated GTR sum occurs, of course, when the main GTR peak at $\approx$19 MeV is included. The RRPA calculation represented by the dashed line includes only positive energy ph configurations. Even extending the sum up to 60 MeV, the total sum amounts only to $\approx$122, that is 8% less than the Ikeda sum rule. The total sum rule $3(N-Z)$ is exhausted by the calculated GT strength only when the relativistic RPA/QRPA space contains ph excitations formed from ground-state configurations of the fully or partially occupied states of positive energy, and the empty negative-energy states from the Dirac sea (solid line in Fig. 7). The corresponding discrete GT spectrum is shown in Fig. 8. Two regions of excitation energies are shown. The panel on the right-hand side contains the positive energy $\pi p - \nu h$ strength, with a pronounced Gamow-Teller peak at $\approx$19 MeV. The left panel displays the negative energy spectrum built from $\pi\alpha - \nu h$ transitions (α denotes a negative energy state). Even though these transitions are much weaker than the GTR, there are many of them and their overall sum represents the strength missing in the positive energy sector. Similar results for the GTR sum rule are also obtained for ^{48}Ca and ^{90}Zr.

For the case of open-shell nuclei we will compare the PN-RQRPA results with experimental data on Gamow-Teller resonances obtained from Sn(^{3}He,t)Sb charge-exchange reactions [40]. The GT strength distribution in ^{118}Sn is shown in Fig. 9. Direct spin-flip transitions $\left(\nu j = l + \frac{1}{2} \rightarrow \pi j = l - \frac{1}{2}\right)$ dominate the high-energy region above 10 MeV. The low-energy tail of the strength distribution corresponds to core-polarization $\left(\nu j = l \pm \frac{1}{2} \rightarrow \pi j = l \pm \frac{1}{2}\right)$, and back spin-flip $\left(\nu j = l - \frac{1}{2} \rightarrow \pi j = l + \frac{1}{2}\right)$ transitions.

The solid curve in Fig. 9 has been calculated without including the $T=0$ proton-neutron pairing in the RQRPA residual interaction. The resulting high-energy GT strength displays pronounced fragmentation. This fragmentation, however, is not induced by coupling to $2p-2h$ configurations (not included in the present version of the RQRPA), rather it is caused by the splitting between different *ph* configurations. GTR configuration splitting (an appearance of two or more collective bumps with comparable intensities in the GTR strength function) was investigated in Ref. [46] in the framework of the shell optical model. For Sn nuclei, in particular, this effect was predicted to occur as the valence neutron start to occupy the level with the highest j in the shell $-h_{11/2}$. The configuration splitting was attributed to the fact that the unperturbed energies of the $(1g^\pi_{7/2})(1g^\nu_{9/2})^{-1}$ and $(1h^\pi_{9/2})(1h^\nu_{11/2})^{-1}$ configurations are almost degenerate. The residual interaction removes this degeneracy and, as a result, the main GT component separates in two distinct peaks. The

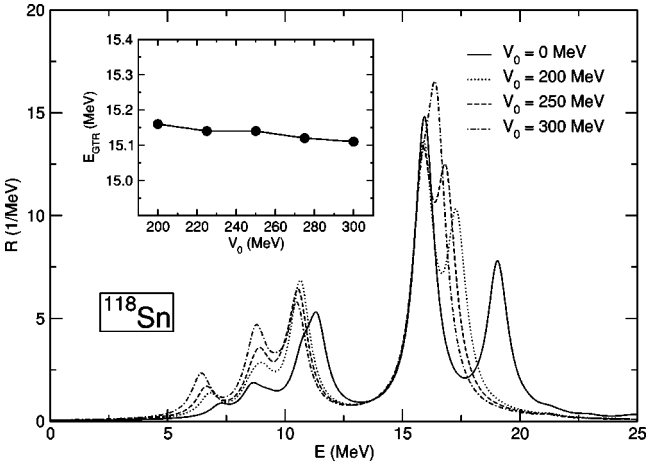

FIG. 9. The Gamow-Teller strength distribution in ^{118}Sn, calculated for different values of the strength parameter of the $T=0$ pairing interaction (14). The insert displays the corresponding calculated centroids of the direct spin-flip GT strength.

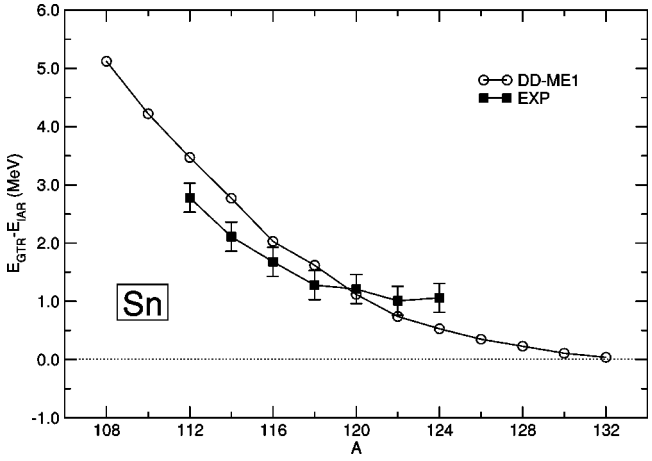

FIG. 10. RHB plus proton-neutron RQRPA results for the energy spacings between the Gamow-Teller resonances and the respective isobaric analog resonances for the sequence of even-even $^{112-124}$Sn target nuclei. The experimental data are from Ref. [40].

ground-state pairing correlations have a strong influence on the occupation of the $1h^{\nu}_{11/2}$ level, and therefore the energy spacing between the two peaks will depend on $T=1$ pairing. For ^{118}Sn the calculated splitting of the GTR was 2.6 MeV [46]. Subsequently, the fragmentation and splitting of the GTR in Sn nuclei was experimentally investigated in Ref. [40]. The theoretically predicted configuration splitting of the main GT component, however, could not be observed, since the total widths of the resonances of 5–6 MeV exceed the predicted splitting. The splitting of the main GT component shown in Fig. 9 (solid line) of $\approx$3 MeV is in agreement with the result of Ref. [46]. In addition, we find a third direct spin-flip component in the region above 10 MeV, predominately based on the configuration $(2d^{\pi}_{3/2})(2d^{\nu}_{5/2})^{-1}$.

The other curves shown in Fig. 9 (dotted, dashed, and dot-dashed) have been calculated with the inclusion of the $T=0$ proton-neutron pairing (14) in the RQRPA residual interaction. In Ref. [26] the overall strength parameter V_0 of the interaction was adjusted to measured half-lives of neutron-rich nuclei in regions where *r*-process path comes closest to the valley of stability: $V_0=230$ MeV near $N=50$ and $V_0=170$ MeV near $N=82$. In the present analysis, however, β-decay half-lives are not calculated and we could not adjust V_0 in this way. The GT strength functions shown in Fig. 9 have been calculated for $V_0=200$, 250, and 300 MeV, respectively. As one would expect, the inclusion of $T=0$ pairing has a strong influence on the low-lying tail of the GT distribution, i.e., on the region that contributes to β decay. Here, however, we are concerned with the main GT component. An important effect that we notice is the disappearance of configuration splitting between the two high-energy peaks. This happens because the $T=0$ pairing interaction does not affect configurations based on the $(1g^{\nu}_{9/2})$ orbital (fully occupied), whereas it lowers configurations based on $(1h^{\nu}_{11/2})$ and $(2d^{\nu}_{5/2})$ (partially occupied). Our calculation therefore shows that the $T=0$ proton-neutron pairing strongly reduces the predicted configuration splitting of the main high-energy GT component. In addition to the main GTR at $\approx$16 MeV, however, part of the strength associated with direct spin-flip transitions is concentrated at $\approx$10 MeV. Another interesting result is that the centroid of the GT strength composed of direct spin-flip transitions $\left(\nu j=l+\frac{1}{2}\rightarrow \pi j=l-\frac{1}{2}\right)$ practically does not depend on the strength of the $T=0$ proton-neutron pp residual interaction. This is shown in the insert of Fig. 9, where we plot the calculated centroid of the direct spin-flip GT strength, as function of the strength parameter V_0. Since we could not use experimental data on the GTR centroid to adjust the strength of the $T=0$ pairing channel, the following illustrative calculations have been performed with $V_0=250$ MeV.

In a recent PN-RQRPA calculation [34] we have shown that the isotopic dependence of the energy spacings between the GTR and IAR provides direct information on the evolution of neutron skin-thickness along the Sn isotopic chain. It has been suggested that the difference between the radii of the neutron and proton density distributions along an isotopic chain, could be determined from the measurement of the excitation energies of the GTR relative to the IAR. The calculation of Ref. [34], however, was performed with the NL3 relativistic mean-field effective interaction. Although NL3 has become a standard in RMF calculations, like many other non-linear meson-exchange effective interactions it has a high nuclear matter asymmetry energy, and consequently it predicts rather large values for neutron density distribution radii. Here we repeat the calculation using the DD-ME1 effective interaction. Among other ground-state nuclear properties, the parameters of DD-ME1 have also been adjusted to experimental data on differences between radii of neutron and proton distributions.

In Fig. 10 we display the calculated differences between the centroids of the direct spin-flip GT strength and the respective isobaric analog resonances for the sequence of even-even Sn target nuclei. For $A=112-124$ the results of RHB plus PN-RQRPA calculation (DD-ME1 density-dependent effective interaction, Gogny $T=1$ pairing, $T=0$ pairing interaction (14) with $V_0=250$ MeV, the Landau-Migdal parameter $g'=0.55$), are compared with experimental data [40].

The calculated energy spacings are in very good agreement with the experimental values. As it has been emphasized in Ref. [34], the energy difference between the GTR and the IAS reflects the magnitude of the effective spin-orbit potential. Many relativistic mean-field calculations have shown that the magnitude of the spin-orbit potential is considerably reduced in neutron-rich nuclei [47], and a corresponding increase of the neutron skin has been predicted. In Fig. 11 the calculated and experimental energy spacings between the GTR and IAS are plotted as a function of the calculated differences between the rms radii of the neutron and proton density distributions of even-even Sn isotopes (upper panel). Notice the uniform dependence of the energy difference between the GTR and IAS on the size of the neutron-skin. This means that, in principle, the value of $r_n - r_p$ can be directly determined from the theoretical curve for a given value of $E_{\mathrm{GT}} - E_{\mathrm{IAS}}$. In the lower panel the calculated differences between neutron and proton rms radii are compared with available experimental data [48]. The agreement between theoretical and experimental values suggests that the neutron-skin thickness can be determined from the measurement of the excitation energies of the GTR relative to IAS.

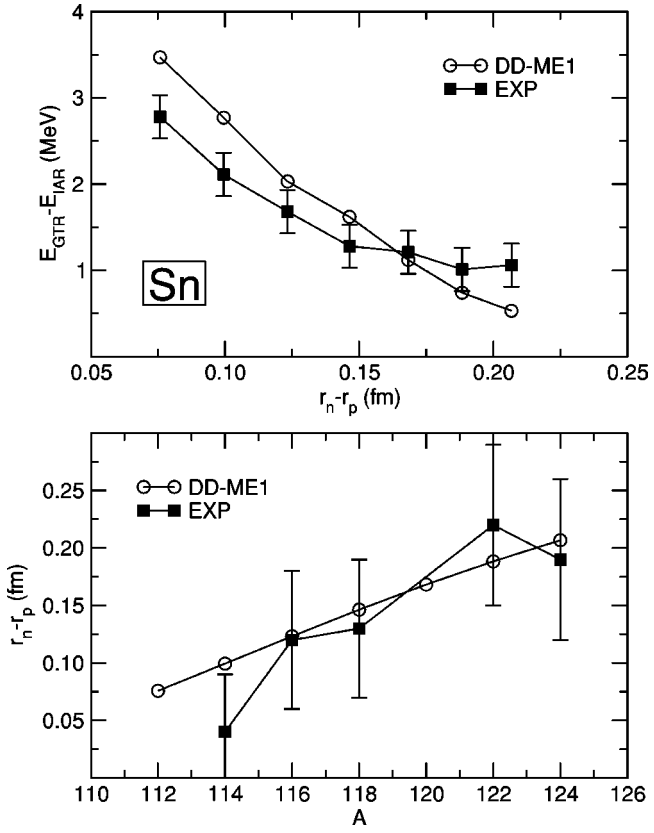

FIG. 11. The proton-neutron RQRPA and experimental [40] differences between the excitation energies of the GTR and IAR, as a function of the calculated differences between the rms radii of the neutron and proton density distributions of even-even Sn isotopes (upper panel). In the lower panel the calculated differences $r_n - r_p$ are compared with experimental data [48].

IV. CONCLUDING REMARKS AND OUTLOOK

In this second part of the work on the RQRPA, we have formulated the proton-neutron RQRPA in the canonical single-nucleon basis of the RHB model, for an effective Lagrangian characterized by density-dependent meson-nucleon couplings. The basic advantage of working in the canonical basis is that, since it diagonalizes the density matrix, the canonical basis is always localized and so it can be used both for bound states and for the positive energy single-particle continuum. This is especially important in the description of low-lying excited states and giant resonances in weakly bound nuclei far from stability. From the practical point of view, it is also considerably simpler to solve the RQRPA equations in the canonical basis, in which the relativistic Hartree-Bogoliubov wave functions can be expressed in the form of BCS-like wave functions.

The inclusion of relativistic effective interactions with explicit density dependence of the meson-nucleon couplings provides an improved description of asymmetric nuclear matter, nuclear ground-states and properties of excited states, especially in nuclei far from stability. The PN-RQRPA model includes both the $T=1$ and $T=0$ pairing channels, and the model space contains pair configurations formed from the fully or partially occupied states of positive energy in the Fermi sea, and the empty negative-energy states from the Dirac sea. It has been shown that the inclusion of configurations built from occupied positive-energy states and empty negative-energy states is essential in order to satisfy model independent sum rules.

The proton-neutron relativistic QRPA provides a natural framework for the description of spin and isospin excitations. In this work the model has been applied to the analysis of charge-exchange modes: isobaric analog resonances and Gamow-Teller resonances. A very good agreement with experimental data has been obtained, both for doubly-closed shell nuclei and for open shell nuclei. The importance of a consistent treatment of pairing correlations has been demonstrated in the example of IAR and GTR in Sn isotopes.

In addition to the IA and GT $0\hbar\omega$ excitations, the (p,n) spectra show clear evidence for the collective spin-flip dipole $(L=1,S=1)$ $1\hbar\omega$ excitation and spin-flip quadrupole $(L=2,S=1)$ $2\hbar\omega$ excitation. The broad (>10 MeV) spin-flip dipole and quadrupole resonances can be interpreted as superpositions of three collective modes with spin-parity $J^\pi = 0^-$, 1^-, 2^-, and $J^\pi = 1^+$, 2^+, 3^+, respectively. It has not yet been possible to experimentally resolve these resonances into the different angular momentum components. Recently it has been suggested that experimental data on charge-exchange spin-dipole resonances can be used to extract information about neutron-skin thickness in neutron-rich nuclei.

The PN-RQRPA will be applied to the study of spin-multipole charge-exchange modes. An interesting question is whether such a self-consistent approach, which starts from the description of the nuclear ground-state, can simultaneously reproduce the dynamics of these high-lying and, in many cases, only weakly collective states. Another important topic will be the calculation of β-decay rates in semimagic neutron-rich nuclei. These nuclei are particularly important

for *r*-process nucleosynthesis. Their lifetimes are rather long and they determine the abundances of stable nuclides. Very neutron-rich nuclei are also very difficult to reach experimentally, and at present the only information on β-decay rates is provided by theoretical calculations. This also emphasizes the importance of the comparison of the present approach with results of non relativistic QRPA calculations.

ACKNOWLEDGMENTS

This work has been supported in part by the Bundesministerium für Bildung und Forschung under Project No. 06 TM 193, and by the Gesellschaft für Schwerionenforschung (GSI) Darmstadt. N.P. acknowledges support from the Deutsche Forschungsgemeinschaft (DFG) under Contract No. SFB 634.

[1] N. Paar, P. Ring, T. Nikšić and D. Vretenar, Phys. Rev. C **67**, 034312 (2003).
[2] T. Nikšić, D. Vretenar, P. Finelli, and P. Ring, Phys. Rev. C **66**, 024306 (2002).
[3] T. Nikšić, D. Vretenar, and P. Ring, Phys. Rev. C **66**, 064302 (2002).
[4] F. Osterfeld, Rev. Mod. Phys. **64**, 491 (1992).
[5] K. Ikeda, S. Fujii, and J. I. Fujita, Phys. Lett. **3**, 271 (1963).
[6] R. R. Doering, A. Galonsky, D. M. Patterson, and G. F. Bertsch, Phys. Rev. Lett. **35**, 1961 (1975).
[7] K. Shimizu, M. Ichimura, and A. Arima, Nucl. Phys. **A226**, 282 (1974).
[8] G. F. Bertsch and I. Hamamoto, Phys. Rev. C **26**, 1323 (1982).
[9] S. Drożdż, V. Klemt, J. Speth, and J. Wambach, Phys. Lett. **166B**, 18 (1986).
[10] M. Ericson, A. Figureau, and C. Thevenet, Phys. Lett. **45B**, 19 (1973).
[11] W. Knüpfer, M. Dillig, and A. Richter, Phys. Lett. **95B**, 349 (1980).
[12] T. Wakasa *et al.*, Phys. Rev. C **55**, 2909 (1997).
[13] E. Caurier, K. Langanke, G. Martinez-Pinedo, and F. Nowacki, Nucl. Phys. **A653**, 439 (1999).
[14] P. B. Radha, D. J. Dean, S. E. Koonin, K. Langanke, and P. Vogel, Phys. Rev. C **56**, 3079 (1997).
[15] J. A. Halbleib and R. A. Sorensen, Nucl. Phys. **A98**, 542 (1967).
[16] N. Van Giai and H. Sagawa, Phys. Lett. **106B**, 379 (1981).
[17] G Colò, N. Van Giai, P. F. Bortignon, and R. A. Broglia, Phys. Rev. C **50**, 1496 (1994).
[18] I. Hamamoto and H. Sagawa, Phys. Rev. C **48**, R960 (1993).
[19] T. Suzuki and H. Sagawa, Eur. Phys. J. A **9**, 49 (2000).
[20] M. Bender, J. Dobaczewski, J. Engel, and W. Nazarewicz, Phys. Rev. C **65**, 054322 (2002).
[21] D. Cha, Phys. Rev. C **27**, 2269 (1983).
[22] M. K. Cheoun, A. Faessler, F. Simkovic, G. Teneva, and A. Bobyk, Nucl. Phys. **A587**, 301 (1995).
[23] J. Engel, P. Vogel, and M. R. Zirnbauer, Phys. Rev. C **37**, 731 (1988).
[24] I. N. Borzov, S. A. Fayans, and E. L. Trykov, Nucl. Phys. **A584**, 335 (1995).
[25] I. N. Borzov, S. A. Fayans, E. Krömer, and D. Zawischa, Z. Phys. A **355**, 117 (1996).
[26] J. Engel, M. Bender, J. Dobaczewski, W. Nazarewicz, and R. Surman, Phys. Rev. C **60**, 014302 (1999).
[27] C. De Conti, A. P. Galeão, and F. Krmpotić, Phys. Lett. B **444**, 14 (1998).
[28] C. De Conti, A. P. Galeão, and F. Krmpotić, Phys. Lett. B **494**, 46 (2000).
[29] H. Kurasawa, T. Suzuki, and N. Van Giai, Phys. Rev. Lett. **91**, 062501 (2003).
[30] Z-Y. Ma, B-Q. Chen, N. Van Giai, and T. Suzuki, nucl-th/0308021.
[31] G. A. Lalazissis, J. König, and P. Ring, Phys. Rev. C **55**, 540 (1997).
[32] S. Krewald, F. Osterfeld, J. Speth, and G. E. Brown, Phys. Rev. Lett. **46**, 103 (1981).
[33] S. Krewald, K. Nakayama, and J. Speth, Phys. Rep. **161**, 103 (1988).
[34] D. Vretenar, N. Paar, T. Nikšić, and P. Ring, Phys. Rev. Lett. **91**, 262502 (2003).
[35] P. Ring and P. Schuck, *The Nuclear Many-Body Problem* (Springer-Verlag, New York, 1980).
[36] J. F. Berger, M. Girod, and D. Gogny, Nucl. Phys. **A428**, 25c (1984).
[37] B. D. Anderson *et al.*, Phys. Rev. C **31**, 1161 (1985).
[38] D. E. Bainum *et al.*, Phys. Rev. Lett. **44**, 1751 (1980).
[39] H. Akimune *et al.*, Phys. Rev. C **52**, 604 (1995).
[40] K. Pham *et al.*, Phys. Rev. C **51**, 526 (1995).
[41] D. J. Horen *et al.*, Phys. Lett. **95B**, 27 (1980).
[42] A. Krasznahorkay *et al.*, Phys. Rev. C **64**, 067302 (2001).
[43] P. G. Reinhard, M. Rufa, J. A. Maruhn, W. Greiner, and J. Friedrich, Z. Phys. A **323**, 13 (1986).
[44] H. Kurasawa, T. Suzuki, and N. Van Giai, Phys. Rev. C **68**, 064311 (2003).
[45] H. Kurasawa and T. Suzuki, Phys. Rev. C **69**, 014306 (2004).
[46] V. G. Guba, M. A. Nikolaev, and M. G. Urin, Phys. Lett. B **218**, 283 (1989).
[47] G. A. Lalazissis, D. Vretenar, W. Pöschl, and P. Ring, Phys. Lett. B **418**, 7 (1998).
[48] A. Krasznahorkay *et al.*, Phys. Rev. Lett. **82**, 3216 (1999).